

3 ROCMAS

ROCMAS is a finite-element code for analysis of coupled THM processes in partially saturated geological media (Noorishad and Tsang, 1996, Rutqvist et al., 2001). In ROCMAS, the Biot (1941) formulation is extended to partially saturated media through Philip and de Vries' (1957) theory for heat- and moisture-flow in soil. This results in a comprehensive coupled THM formulation for partially saturated geological media that includes the coupled processes shown in Figure 2.

In ROCMAS, solid, liquid, and gas phases are considered. However, it is assumed that the gas pressure P_g is constant and equal to atmospheric pressure throughout the porous medium. As a consequence, vapor transport occurs only through molecular diffusion driven by a gradient in vapor concentration. The heat transfer may take place through conduction over all phases and by advection with water in both liquid and gas phases.

For the analysis of the FEBEX *in situ* test, a soil mechanics state-surface model was implemented. This state-surface approach provides a better representation of bentonite behavior under partially saturated conditions than a single effective stress approach. The logarithmic state surface model proposed by Lloret and Alonso (1985) was adopted in this analysis. In their model, void ratio (e) is a function of both net mean stress, ($\sigma_m'' = \sigma_m - p_g$, where $\sigma_m =$ total mean stress and p_g is gas pressure) and suction ($s = p_g - p_l$, where p_g and p_l is gas and liquid pressures, respectively).

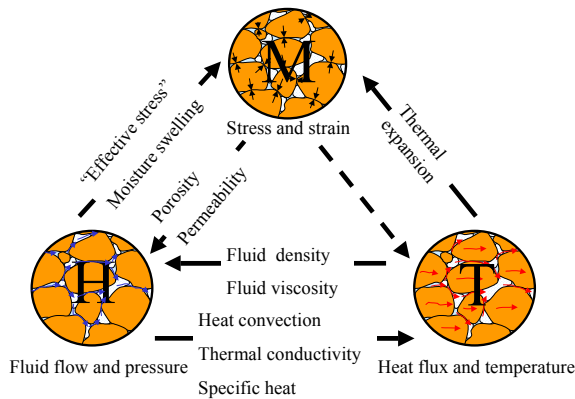


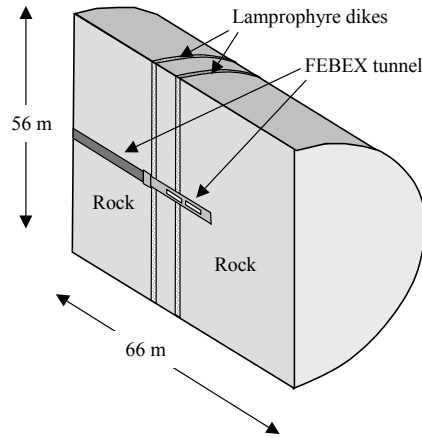
Figure 2. Coupled THM processes in unsaturated geological media simulated by the ROCMAS code

4 FEBEX MODEL

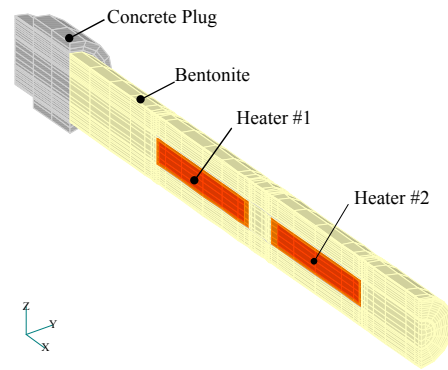
A three-dimensional fully coupled THM analysis of the FEBEX *in situ* test was carried out for the first 1,000 days of heating. Model geometry and material properties are presented in the next two subsections.

4.1 Geometry

A half-symmetrical three-dimensional model was discretized as shown in Figure 3a. The model includes two highly permeable lamprophyre dykes that intersect the FEBEX tunnel (Figure 3). These zones are included in the model because wetting rate of the bentonite might depend on the local permeability of the surrounding rock. The engineered materials included in the model are a concrete plug, the bentonite barrier, a steel liner (around the heaters), and the heater canisters (Figure 3b).



(a) Entire model of FEBEX



(b) Detailed view of the near field materials

Figure 3. Finite element model of FEBEX

4.2 Material properties

The material properties were obtained from various field and laboratory tests that were performed before the emplacement of the buffer and heaters. For example, the inflow into the open drift was utilized to calibrate the *in situ* hydraulic properties of the rock mass and Lamprophyre dykes. Moreover, several laboratory tests were utilized for numerical back-analyses of coupled THM properties of the bentonite. The properties of the bentonite and rock are listed in Tables 1 and 2.

Some of the material properties listed in Table 1 are given in the form of functions. The water-retention curve of the bentonite is described by a modified van Genuchten (1980) function as:

$$S = 0.01 + (0.99) \left[1 + (s/35)^{1.43} \right]^{-0.30} \left[1 - s/4000 \right]^{1.5} \quad (1)$$

where S is liquid saturation and s is suction.

The thermal conductivity is a function of saturation according to:

$$\lambda_m = 1.28 - \frac{0.71}{1 + e^{(S-0.65)/0.1}} \quad (2)$$

and specific heat is a function of temperature according to:

$$c_s = 1.38T + 732.5 \quad (3)$$

The state surface model for this particular bentonite's mechanical behavior is defined as:

$$e = 1.03 - 0.49 \log \sigma_m'' - 0.17 \log s + 0.23 \log \sigma_m'' \log s \quad (4)$$

As shown in Table 2, the properties of the Lamprophyre properties and the surrounding rock are the same except for permeability and thermal conductivity. The mechanical rock-mass properties are obtained from the geological description of the Grimsel Test Site (Kneussen et al., 1989). Significantly, the Young's modulus of the rock mass was reduced to 70% of its value for intact rock.

Table 1. Material properties of the bentonite barrier used in modeling the FEBEX heater test

Parameter	Value
Dry density, [kg/m ³]	1.6·10 ³
Porosity, [-]	0.41
Saturated permeability, [m ²]	2.0·10 ⁻²¹
Relative permeability, k_{r1}	$k_{r1} = S^3$
Water retention	Equation (1)
State surface	Equation (4)
Poisson ratio, [-]	0.35
Thermal expan. coeff., [1/°C]	1.0·10 ⁻⁵
Dry specific heat, [J/kg·°C]	Equation (3)
Thermal cond., [W/m·°C]	Equation (2)
Flow times tortousity factor	0.8
Thermal diffusion factor	2.0

Table 2. Material properties of the rock mass used in modeling the FEBEX heater test

Parameter	Value
Density, [kg/m ³]	2700
Porosity, [-]	0.01
Biot's constant, α [-]	1.0
Young's Modulus, [GPa]	35
Poissons ratio, [-]	0.3
Specific heat, [J/kg·°C]	800
Thermal conductivity, [W/m·°C]	3.6
Thermal expan, coefficient [1/°C]	8.21·10 ⁻⁶
Vertical permeability, [m ²]	5×10 ⁻¹⁸
Horizontal permeability, [m ²]	5×10 ⁻¹⁹
Van-Genuchten's parameter, P_0 [MPa]	1.47
Van Genuchten's parameter, β	2.47
Lamprophyre permeability, [m ²]	1.1×10 ⁻¹⁷
Lamprophyre thermal cond. [W/m·°C]	2.45

5 SIMULATION RESULTS

The simulation of the FEBEX *in situ* test included both pre-heating and heating periods, as shown in Figure 4. The simulation began eight months before heating to take into account the wetting of the bentonite during the experimental setup. After the initiation of heating, the heater power was increased step-wise during the first 53 days. Then the power of each heater was individually controlled by a constant heater temperature of 100°C. The simulated heater power shown in Figure 4 is slightly lower than the measured one.

In the following subsections, simulated and measured system responses are compared at selected monitoring points within the bentonite barrier.

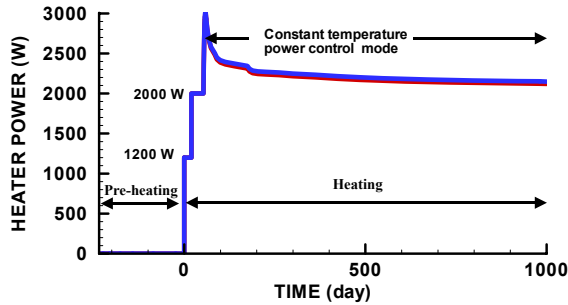


Figure 4. Simulated heater power as a function of time for each heater. A constant temperature mode is implemented after 53 days

5.1 Results of temperature

Figure 5 presents simulated temperature in the bentonite barrier after 1,000 days. The figure shows the location of the hottest point on the heater surface, which is kept at a constant temperature of 100°C. At the drift wall the temperature reaches a maximum of about 40–50°C, giving rise to a thermal gradient of about 80 to 90°C/m.

In Figure 6, simulated and measured temperature evolutions are compared at monitoring point D1G, located near the drift wall. The good agreement between simulated and measured temperature shown in Figure 6 is typical. This confirms that temperature can be very well predicted by numerical analysis in this type of environment.

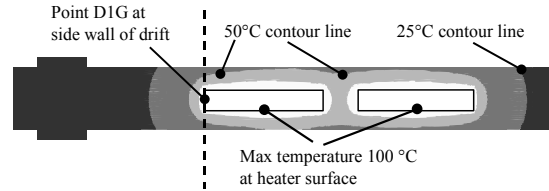


Figure 5. Simulated temperature contour after 1,000 days of heating

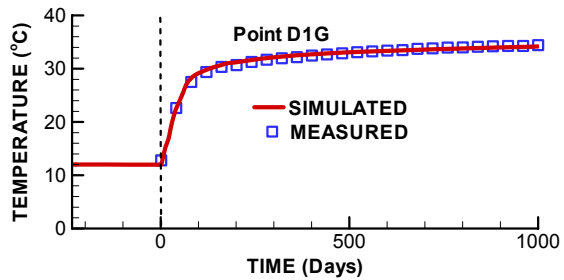


Figure 6. Simulated and measured temperature evolution in point D1G located at the drift wall

5.2 Results of moisture content

Figure 7 shows simulated liquid saturation after 1,000 days of heating. The dark contours in Figure 7 indicate zones where wetting of the bentonite have taken place. The simulated wetting has begun already before heating through water infiltration from the fully saturated rock. The light contours in Figure 7 indicate that the drying zone has taken place near each of the heaters. This drying is caused by evaporation and transport of vapor along the thermal gradient away from the heaters. Another observation in Figure 7 is that the wetting of the bentonite progresses uniformly all around the drift without any visible effects from the high permeability Lamprophyres.

Figure 8 presents simulated and measured evolutions of the moisture content (relative humidity) at three points located along a vertical monitoring section between the two heaters (HG, HC and HH in Figure 7). Figure 8 shows that the wetting of the bentonite starts at the drift wall (Point HG located a few centimeters from the rock surface) as soon as the bentonite is installed in that section. At this monitoring point, the relative

humidity has increased to about 80–90% at heater turn-on (time = 0 in Figure 8).

At point HH, condensation of vapor caused a slight wetting during the first 100 days. For the period between 100 to 300 days, the water content decreased slightly because of drying induced by the heat. After 300 days, the relative humidity increased again as a result of capillary driven liquid flow from the outer regions of the bentonite.

At point HC—located halfway between the heater and the drift wall—the moisture content increased gradually as a result of infiltration from the fully saturated rock.

Figure 8 indicates that the evolution of relative humidity was reasonable well predicted by the numerical analysis.

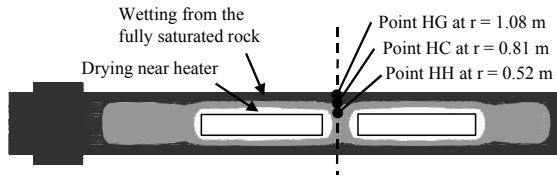


Figure 7. Simulated contour of liquid saturation in the bentonite buffer after 1,000 days of heating: Dark and light contours indicate wetting and drying, respectively

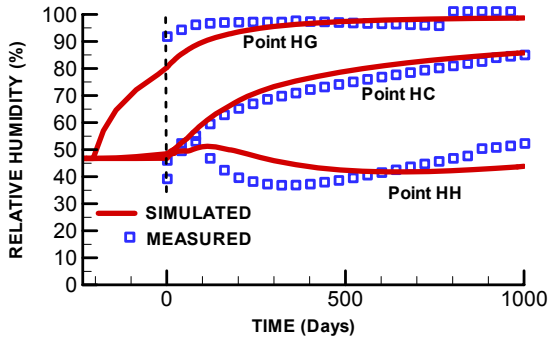


Figure 8. Simulated and measured evolution of relative humidity at points HG, HC and HH with locations shown in Figure 7

5.3 Results of Stress

Figure 9 presents simulated contours of intermediate compressive-principal-stress at 1,000 days. The figure shows that compressive stress caused by swelling pressure has developed at the drift wall, especially at the front end of the tunnel, where the bentonite blocks were first installed.

Figure 10 presents simulated and measured evolution of stress normal to the drift wall at two locations (E2G2 and B2G in Figure 9). The simulated stress began to develop as soon as the wetting commenced and increased to about 2 to 2.5 MPa at 1,000 days. The measured stress indicates that the swelling stress might not have begun to develop until several months after heater turn-on. This delay in the development of swelling stress was a common observation at many monitoring points in the bentonite barrier at FEBEX.

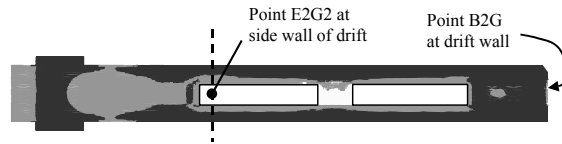


Figure 9. Simulated contour of intermediate principal stress in the bentonite buffer after 1,000 days of heating: dark contour indicates the highest compressive stress (2 to 3 MPa), whereas light contour indicates the lowest compressive stress (0 to 1 MPa)

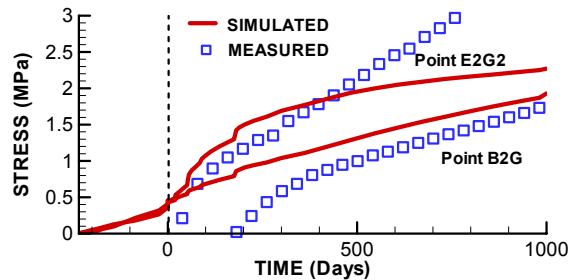


Figure 10. Simulated and measured evolution of radial stress at points E2G2 and B2G, with locations shown in Figure 9

6 DISCUSSION

The general agreement between simulated and measured THM responses at FEBEX indicates that coupled THM processes are well represented in the ROCMAS code.

The good agreement between simulated and measured temperature indicates that thermal responses can be predicted with high confidence. This is a consequence of heat conduction being the dominant mode of heat transport. If the thermal conductivity and specific heat are accurately represented in the model, the temperature responses should be well predicted.

The evolution of the moisture content was reasonably well predicted both in trends and magnitudes. Moreover, results from the modeling and field measurements at FEBEX indicate that the presence of highly permeable Lamprophyres (Figure 3a) did not have a significant impact on the wetting of the buffer. This shows that the wetting of buffer was controlled by the hydraulic properties of the bentonite barrier with unrestricted water supply from the surrounding rock mass.

The evolution of swelling pressure in the buffer was generally underestimated during the first several hundred days. The measured delay in the swelling stress at FEBEX was probably caused by the existence of gaps between the bentonite blocks. It appears that the swelling stress in the buffer began to develop after a few months when the gaps had closed. These gaps were not considered in our numerical model, and consequently the simulated swelling stress developed much earlier.

7 CONCLUSIONS

The numerical model ROCMAS was applied to predict coupled THM processes in a bentonite barrier at the FEBEX *in situ* test. The results indicate that numerical modeling can provide highly reliable predictions for temperature distribution, and reasonably reliable predictions for moisture flow and stress in a bentonite barrier. Moreover, field observations and modeling shows that resaturation of the buffer was controlled by the properties of the bentonite barrier whereas the permeability of the rock was sufficiently high to act as an unrestricted water source. Therefore, the wetting of the bentonite took place uniformly from the rock and was not impacted by the permeability difference between the Lamprophyres dykes and surrounding rock.

The evolution of stress in the bentonite barrier at FEBEX was affected by the existence of gaps between the pre-fabricated bentonite blocks. The swelling pressure did not develop until moisture swelling of the bentonite blocks had closed the gaps completely.

ACKNOWLEDGEMENTS

Reviews and comments by Hui-Hai Lui and Dan Hawkes, Lawrence Berkeley National Laboratory are much appreciated. Financial support was provided by a grant from the Swedish Nuclear Power Inspectorate (SKI).

REFERENCES

- Biot, M. A. 1941. *General theory of three dimensional consolidation*. J. Applied Physics 12: 155-164.
- van Genuchten, M. T., 1980. *A closed-form equation for predicting the hydraulic conductivity of unsaturated soils*. Soil Sci Soc Am J 44: pp. 892-898.
- Keusen H.R., Ganguin J., Schuler P. & Buletti M, Grimsel. 1989. *Test Site-Geology*. NAGRA, NTB 87-14E.
- Lloret A. & Alonso E.E. 1985. *State surfaces for partially saturated soils*. Proc 11th Int Conf Soil Mech Fdn Engng, San Francisco, Vol. 2, pp. 557-562.
- Noorishad, J. & Tsang, C.-F. 1996. *ROCMAS simulator; A thermohydromechanical computer code*. In O. Stephansson, L. Jing & C.-F. Tsang, (Eds), *Coupled thermo-hydro-mechanical processes of fractured media*: 551-558. Elsevier.
- Philip, J.R. & de Vries, D.A. 1957. *Moisture movement in porous material under temperature gradients*. EOS Trans., AGU. 38: 222-232.
- Rutqvist, J., Borgesson, L., Chijimatsu, M., Kobayashi, A., Nguyen, T.S., Jing, L., Noorishad, J. & Tsang, C.-F. 2001. *Thermohydromechanics of partially saturated geological media: governing equations and formulation of four finite element models*. Int. J. Rock. Mech. Min. Sci. 38(1): 105-127.